Precambrian Research 275 (2016) 35–47

Contents lists available at ScienceDirect

Precambrian Research

journal homepage: www.elsevier.com/locate/precamres

Crustal evolution of the Eastern Block in the North China Craton: Constraints from zircon U–Pb geochronology and Lu–Hf isotopes of the Northern Liaoning Complex

Meiling Wu[a,b], Shoufa Lin[a,c,*], Yusheng Wan[b], Jian-Feng Gao[d]

[a] Department of Earth and Environmental Sciences, University of Waterloo, Waterloo, Ontario N2L 3G1, Canada
[b] Beijing SHRIMP Center, Institute of Geology, Chinese Academy of Geological Sciences, Beijing 100037, China
[c] School of Resources and Environment, Hefei University of Technology, Hefei 230026, China
[d] State Key Laboratory of Ore Deposit Geochemistry, Institute of Geochemistry, Chinese Academy of Sciences, Guiyang 550002, China

ARTICLE INFO

Article history:
Received 6 November 2015
Received in revised form 7 December 2015
Accepted 15 December 2015
Available online 25 December 2015

Keywords:
Zircon U–Pb dating
Hf isotopes
Neoarchean
Crustal evolution
North China Craton
Northern Liaoning Complex

ABSTRACT

The Northern Liaoning Complex in northeastern China constitutes an important component of the Eastern Block in the North China Craton. The major lithologies consist of Archean granitoid gneisses with minor supracrustal rocks occurring as tectonic lenses. This study presents zircon Lu–Hf isotopic data for the first time as well as new SHRIMP zircon U–Pb data of the major lithologies from the Northern Liaoning Complex, in order to elucidate the crustal evolution of the complex and provide new constraints on the Neoarchean crustal evolution of the Eastern Block in the North China Craton. Magmatic zircon U–Pb data from this study show that the protolith magmas of the supracrustal rocks and granitoid gneisses were generated during ~2.55–2.50 Ga. Metamorphic zircons document consistent metamorphic ages at 2.49–2.48 Ga, suggesting a regional metamorphic event immediately after the magmatism at the end of the Neoarchean in the Northern Liaoning Complex. Inherited/detrital zircons of 2.79–2.60 Ga suggest possible existence of ancient crust in this region. Zircon Lu–Hf isotopic compositions show that the magmatic zircons have variable $\varepsilon_{Hf}(t)$ values from −4.0 to +9.0 with depleted mantle model ages of 3.6–2.5 Ga, of which most $\varepsilon_{Hf}(t)$ values are positive with a model age peak at 2.9–2.7 Ga. These zircon Hf signatures reveal major juvenile crustal growth with additions of older crustal materials during 2.9–2.7 Ga, and a crustal reworking event with minor juvenile additions at 2.6–2.5 Ga in the studied area. Integrated with previous data from other Neoarchean complexes in the Eastern Block, both the major juvenile crustal growth during 2.9–2.7 Ga and the strong crustal reworking at 2.6–2.5 Ga contribute to the extensive Neoarchean crust formation of the Eastern Block in the North China Craton. The North China Craton share similar Neoarchean continental crustal evolution to other cratons in the world, though it is distinctively featured by intensive tectonothermal overprinting at the end of the Neoarchean.

1. Introduction

Numerous geochronological and isotopic data from different cratons all over the world have revealed several major crust-forming stages at 3.5–3.2 Ga, 2.8–2.7 Ga and 2.6–2.5 Ga, producing voluminous tonalite-trondhjemite-granodiorite (TTG) rocks and volcanic rocks, which constitute the majority of the continental crust (Hawkesworth and Kemp, 2006; Condie and Aster, 2010; Condie et al., 2009). Of these crust formation events, the ~2.8–2.7 Ga tectonothermal event is of global significance, as it resulted in a great amount of continental crust formation over a short period in many cratons, such as in the Superior Craton (Beakhouse et al., 2011; Percival et al., 2006), South Africa Craton (Kröner et al., 1999; Poujol et al., 2003), Western Greenland Craton (Crowley, 2002), Baltic craton (Bibikova et al., 2005), Wyoming Craton (Rino et al., 2004) and Yilgarn Craton (Bateman et al., 2001). Comparatively, the ~2.6–2.5 Ga (end-Archean) tectonothermal events have only been identified in a few cratons, such as the Antarctic Craton (Black et al., 1991), South India Craton (Jayananda et al., 2000) and North China Craton (NCC) (e.g. Zhao et al., 2001, 2005).

The North China Craton (NCC) is a key area to address the end-Neoarchean tectonothermal event due to the good exposure and accessibility of voluminous late Neoarchean (2.6–2.5 Ga)

* Corresponding author at: Department of Earth and Environmental Sciences, University of Waterloo, 200 University Avenue West, Waterloo, Ontario N2L 3G1, Canada. Tel.: +1 5198884567x36557; fax: +1 519 746 7484.
E-mail address: shoufa@uwaterloo.ca (S. Lin).

http://dx.doi.org/10.1016/j.precamres.2015.12.013
0301-9268/

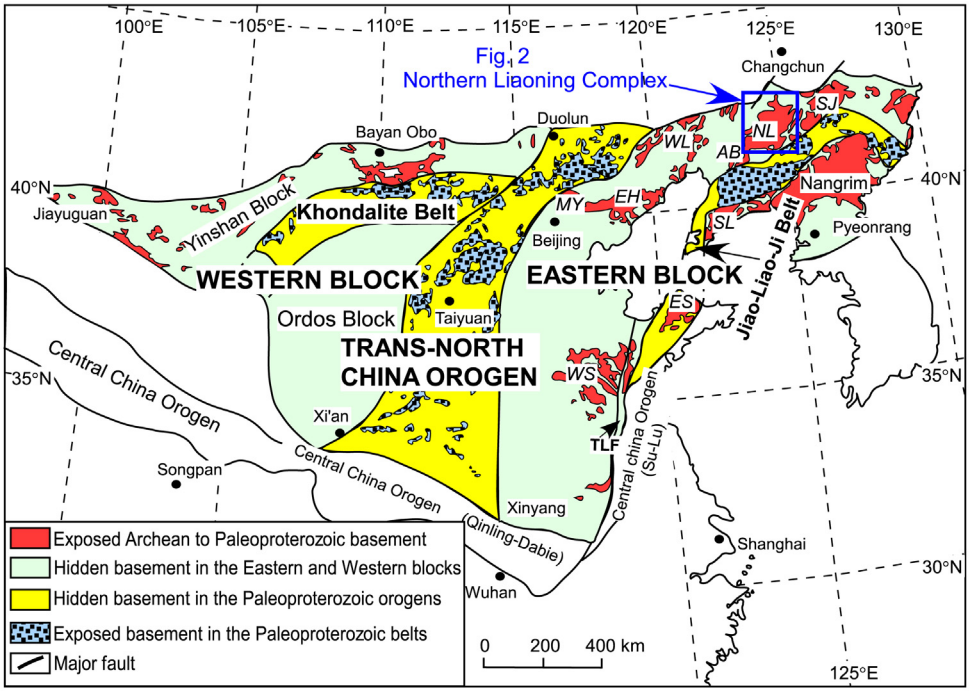

Fig. 1. Tectonic subdivision of the North China Craton (modified after Zhao et al., 2005). Abbreviations: MY = Miyun; EH = Eastern Hebei; WS = Western Shandong; ES = Eastern Shandong; SL = Southern Liaoning; NL = Northern Liaoning; WL = Western Liaoning; SJ = Southern Jilin; AB = Anshan-Benxi; TLF = Tancheng-Lujiang fault.

basement rocks (Santosh, 2010; Zhai, 2014; Zhao and Cawood, 2012). Major advancements on the formation and evolution of the Precambrian basement of the NCC have led to a broad consensus that the NCC is formed by accretion and amalgamation of several micro-continental blocks (Lu et al., 2008; Kusky and Li, 2003; Santosh, 2010; Wilde and Zhao, 2005; Zhai, 2014; Zhao et al., 1998, 2001, 2012). Based on a widely-accepted tectonic model proposed by Zhao et al. (2001, 2005, 2012), these Archean micro-continental blocks were amalgamated along three major Paleoproterozoic mobile belts, namely the Trans-North China Orogen, the Khondalite Belt and the Jiao-Liao-Ji Belt (Fig. 1; Wilde and Zhao, 2005; Zhao et al., 2001, 2005, 2012). Extensive investigations have been carried out on these mobile belts to reveal the collisional history (e.g. Guo et al., 2002, 2005; Li et al., 2005, 2006, 2010; Santosh, 2010; Tam et al., 2011; Wilde and Zhao, 2005; Yin et al., 2009, 2011; Zhang et al., 2006, 2007, 2009; Zhao et al., 2001, 2005; Zhou et al., 2008). However, the pre-collisional history of the Archean micro-continental blocks in the NCC is relatively poorly investigated, which has hampered a further understanding of the Archean crustal evolution of the craton.

Available geochronological data indicate that most of the Neoarchean basement rocks in the Eastern Block were formed during ~2.6–2.5 Ga, while only a few were formed during 2.8–2.7 Ga (Wan et al., 2011; Tang et al., 2007; Liu et al., 2013; Wu et al., 2014a,b). All these basement rocks experienced a large-scale regional metamorphism at ~2.50 Ga with anticlockwise *P–T* paths (Ge et al., 2003; Geng et al., 2006, 2012; Grant et al., 2009; Liu et al., 2011; Kröner et al., 1998; Shen et al., 2007; Wu et al., 2012, 2013b, 2014a,b; Yang et al., 2008). This significant end-of-Neoarchean tectonothermal event over the NCC makes the NCC distinct from most other Archean cratons that are characterized by ~2.8–2.7 Ga tectonothermal events (Condie et al., 2009). Although 2.8–2.7 Ga rocks have also been identified locally in the NCC, it remains equivocal whether or not the entire Eastern Block underwent an extensive crustal growth event at 2.8–2.7 Ga, like most other cratons in the world. Extensive investigations have been carried out in the central part of the Eastern Block, including Western Shandong (Jahn et al., 1988; Peng et al., 2012; Wan et al., 2010, 2011, 2012; Wang et al., 2009, 2013a,b, 2014), Eastern Shandong (Tang et al., 2007; Jahn et al., 2008; Liu et al., 2013; Wu et al., 2014a,b,c; Zhou et al., 2008) and Eastern Hebei Complexes (Bai et al., 2015; Guo et al., 2013; Nutman et al., 2011; Yang et al., 2008), whereas study on the crust evolution of the Northern Liaoning Complex in the northeastern part of the Eastern Block is limited. In this study, we carried out LA-ICP-MS zircon Lu–Hf isotopic study for the first time in addition to SHRIMP zircon U–Pb dating on the major lithological units from the Northern Liaoning Complex. A synthesis of previous studies and our new data will not only place geochronological constraints on the tectonothermal framework of the Northern Liaoning Complex, but also provide important insights into understanding the Neoarchean crustal evolution of the Eastern Block in the NCC.

2. Regional geology

The Archean basement is widely exposed in the Eastern Block of the NCC as several complexes as shown in Fig. 1, including the Eastern Hebei, Miyun, Western Shandong, Eastern Shandong, Western Liaoning, Northern Liaoning and Southern Jilin complexes. In the northeastern part of the Eastern Block, the Northern Liaoning and the Southern Jilin complexes comprise the Longgang Block, which amalgamated with the Nangrim Block along the Jiao-Liao-Ji Belt during the Paleoproterozoic (Fig. 1; Zhao et al., 2005).

The Northern Liaoning Complex is located in Liaoning Province in northeastern China and is mainly exposed in the Qingyuan, Fushun, and Xinbin areas (Fig. 1). It is in tectonic contact with the Central Asian Orogenic Belt to the north and the Jiao-Liao-Ji belt to the south. The complex includes large volumes of granitoid gneisses of TTG composition and minor mafic to felsic metavolcanic or metasedimentary rocks, commonly known as the "Qingyuan group" in Chinese literature. They experienced medium-high grade metamorphism and multi-phase deformation. Minor post-tectonic potassium-rich granites and charnockites are also present. The supracrustal rocks comprise of serpentinite, amphibolite, granulite, felsic and pelitic gneisses, hosting plenty of mineral resources, such

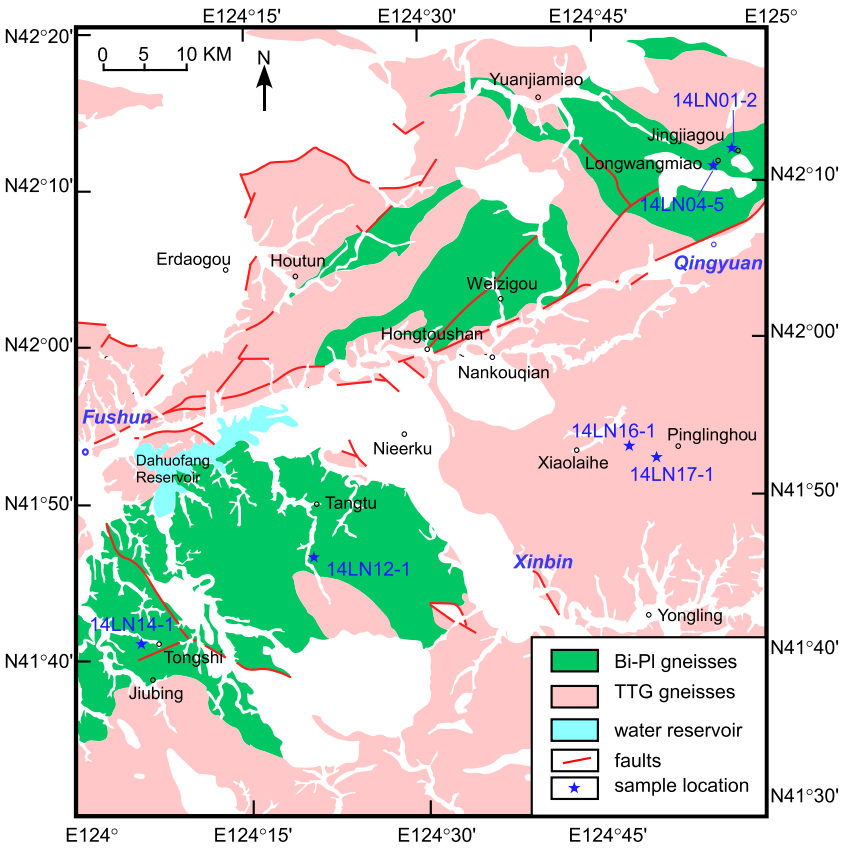

Fig. 2. Simplified geological map of the Northern Liaoning Complex (modified after Shen et al., 1994).

as iron, copper, zinc and gold (Li et al., 1999; Shen et al., 1994). Some scholars consider that the Northern Liaoning Complex represents a typical Archean granite-greenstone terrain (Peng et al., 2015; Shen et al., 1994; Wan et al., 2005b; Zhai et al., 1985; Zhai, 2014), although the grade of metamorphism is significantly higher (upper amphibolite or granulite facies, as opposed to typically greenschist facies in most granite-greenstone terranes elsewhere).

Limited geochronological studies have been carried out in the Northern Liaoning Complex. Previously, Ar–Ar and Sm–Nd ages of minerals and whole-rock samples and multigrain zircon U–Pb analyses gave Mesoarchean to early Neoarchean ages of 2.9–2.6 Ga for the complex (Li and Shen, 2000; Peucat and Jahn, 1986; Shen et al., 1994; Zhai et al., 1985). However, recent studies using in situ zircon U–Pb dating have revealed that its majority were formed during late Neoarchean between 2.56 and 2.51 Ga and metamorphosed during 2.52–2.47 Ga (Bai et al., 2014; Grant et al., 2009; Wan et al., 2005a). Besides, on the basis of previous geochemical data, different tectonic models for the Northern Liaoning Complex have been proposed. Zhai et al. (1985) suggested the supracrustal rocks ("greenstones") were of volcanic origin and erupted in a continental rift setting above a hotspot, whereas Wan et al. (2005b) proposed that this complex was formed in a continental arc setting followed by arc collision. Most recently, Wu et al. (2013b) favored a mantle plume model to explain the metamorphic evolution of the Northern Liaoning Complex, which is characterized by a counter-clockwise metamorphic *P–T* path with an isobaric cooling process.

3. Petrology and sampling

Six representative samples of different lithologies from the Northern Liaoning Complexes were selected for zircon U–Pb dating and Lu–Hf isotopic analysis. The samples include two granulite samples (14LN01-2 and 14LN17-1), one garnet-amphibolite sample (14LN12-1), one garnet-hornblende-biotite-plagioclase gneiss sample (14LN04-5), and two garnet-biotite-plagioclase gneiss samples (14LN14-1 and 14LN16-1). Sample locations are shown in Fig. 2 and summarized in Table 1.

3.1. Sample 14LN01-2

This coarse-grained granulite occurs as big individual enclaves within the weathered hosting gneisses (Fig. 3a). The major mineral phases include orthopyroxene (20%), hornblende (10%), biotite

Table 1
Summary of sample locations.

Sample	Lithology	Locality	GPS
14LN01-2	Granulite	Jingjiagou village	N42°11′43.26″, E124°57′4.32″
14LN17-1	Granulite	Pinglinghou village	N41°52′41.94″, E124°50′13.32″
14LN12-1	Grt-amphibolite	Tangtu village	N41°46′11.76″, E124°20′7.68″
14LN04-5	Grt-Hb-Bt-Pl gneiss	Longwangmiao village	N42°10′54.18″, E124°55′33.42″
14LN14-1	Grt-Bt-Pl gneiss	Tongshi village	N41°41′03.36″, E124°6′18.6″
14LN16-1	Grt-Bt-Pl gneiss	Xiaolaihe iron mine	N41°52′53.64″, E124°47′53.88″

Mineral abbreviations: Bt – biotite; Grt – garnet; Hb – hornblende; Pl – plagioclase.

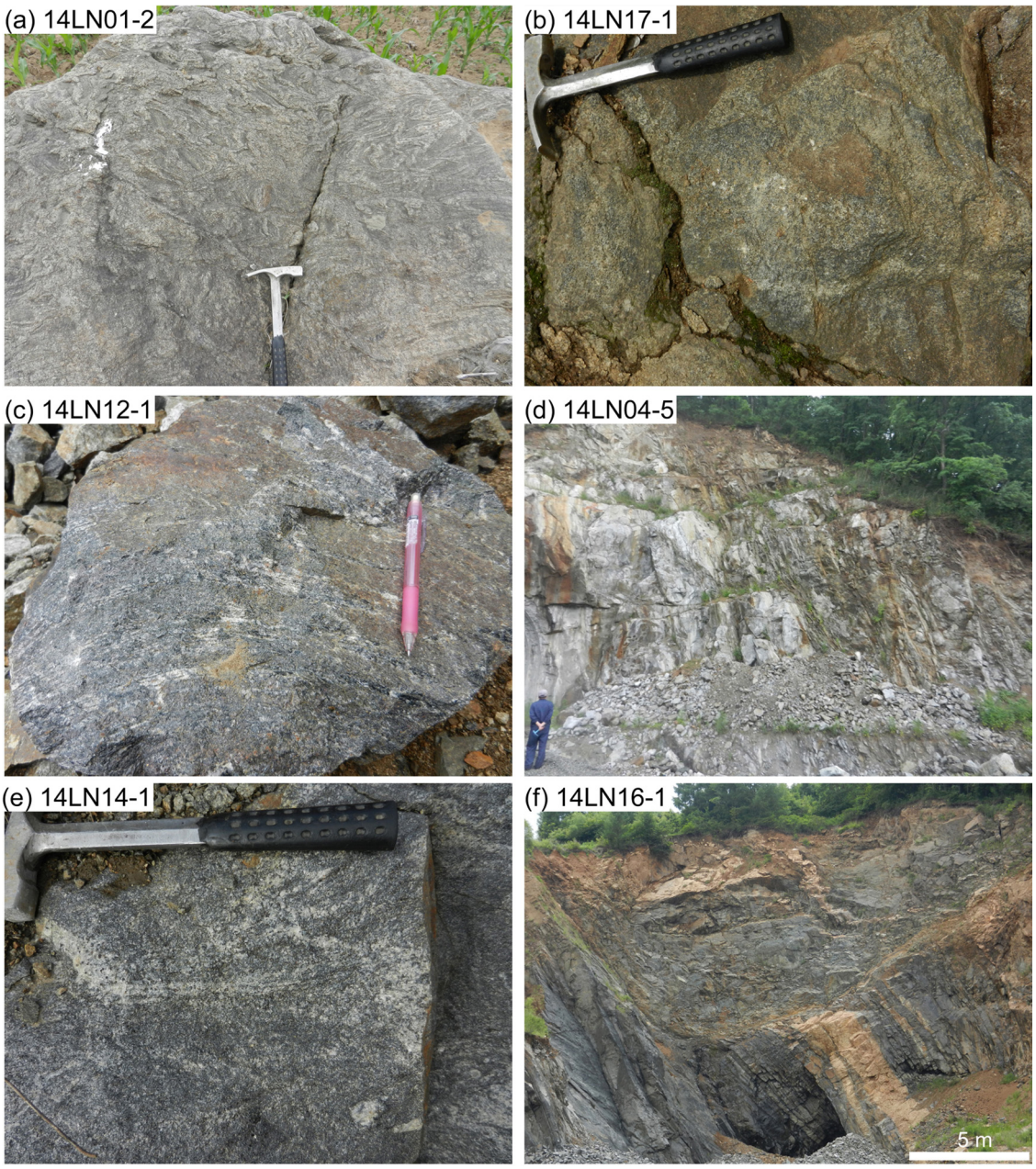

Fig. 3. Field photographs of major lithologies of the Northern Liaoning Complex. (a) Granulite (sample 14LN01-1); (b) granulite (sample 14LN17-1); (c) garnet-amphibolite (sample 14LN12-1); (d) garnet-hornblende-biotite-plagioclase gneiss (sample 14LN04-5); (e) garnet-biotite-plagioclase gneiss (sample 14LN14-1), and (f) garnet-biotite-plagioclase gneiss (sample 14LN16-1).

(15%), plagioclase (45%) and quartz (10%). Most rims of orthopyroxene are replaced by hornblende, some of which are further replaced by biotite (Fig. 4a). In the same outcrop, garnet is locally present due to compositional heterogeneity. The occurrence of orthopyroxene and garnet suggests granulite facies metamorphism in this region.

3.2. Sample 14LN17-1

This sample is a medium-coarse-grained garnet-bearing granulite. It occurs as a massive enclave within the host felsic gneisses (Fig. 3b). The mineral assemblage is garnet (10%) + orthopyroxene (10%) + hornblende (15%) + biotite (5%) + plagioclase (40%) + quartz (20%) + magnetite (5%) (Fig. 4b). Rims of orthopyroxene are commonly replaced by retrogressive hornblende or biotite.

3.3. Sample 14LN12-1

This garnet-bearing amphibolite shows good gneissosity (Fig. 3c) and consists mainly of garnet (5%) + biotite (15%) + hornblende (25%) + plagioclase (40%) + quartz (15%) + magnetite (5%) (Fig. 4c). Hornblende locally retrogrades to biotite, resulting in the decrease of hornblende content and the increase of biotite content.

3.4. Sample 14LN04-5

This medium-grained garnet-biotite-plagioclase gneiss sample was collected near the abandoned Longwangmiao gold mine to the north of the Qingyuan County (Fig. 2). The rock shows good gneissosity in the field (Fig. 3d), with a mineral assemblage of garnet (5%) + biotite (7%) + muscovite (3%) + plagioclase (60%) + quartz

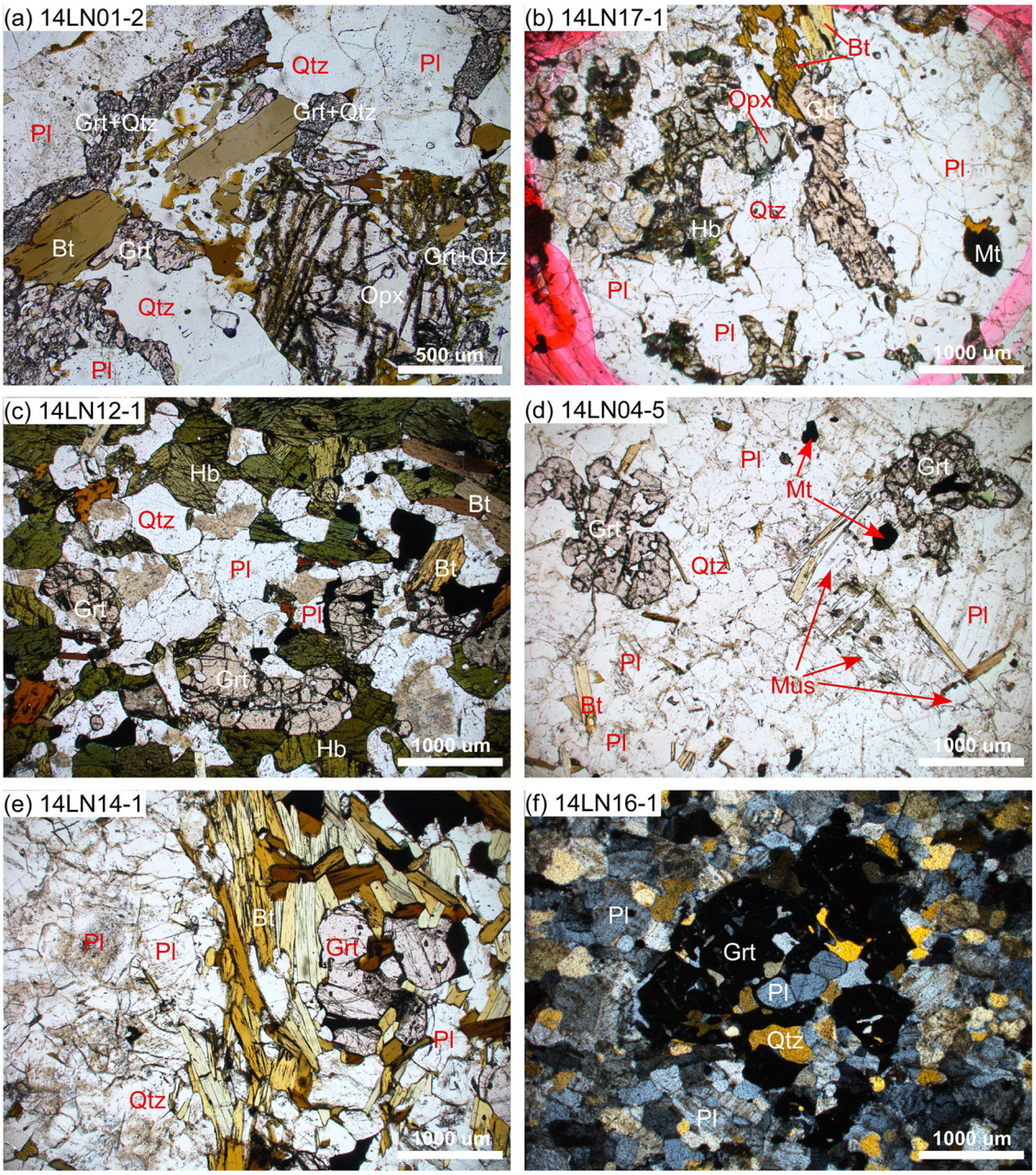

Fig. 4. Photomicrographs of major lithologies of the Northern Liaoning Complex. (a) Granulite (sample 14LN01-1); (b) granulite (sample 14LN17-1); (c) garnet-amphibolite (sample 14LN12-1); (d) garnet-hornblende-biotite-plagioclase gneiss (sample 14LN04-5); (e) garnet-biotite-plagioclase gneiss (sample 14LN14-1); and (f) garnet-biotite-plagioclase gneiss (sample 14LN16-1). Abbreviations: Bt = biotite; Cpx = clinopyroxene; Grt = garnet; Hb = hornblende; Opx = orthopyroxene; Pl = plagioclase; Qtz = quartz.

(25%) + magnetite (5%) (Fig. 4d). Muscovite is considered to be a later alteration product from biotite.

3.5. Sample 14LN14-1

This sample is a coarse-grained garnet-biotite-plagioclase gneiss. The rock shows weak gneissosity (Fig. 3e) and consists of garnet (15%) + biotite (30–40%) + plagioclase (30%) + quartz (20%) + magnetite (5%) (Fig. 4e). Garnet is commonly present as coarse-grained porphyroblast (Fig. 4e). Oriented biotite aggregates define a weak foliation (Fig. 4e).

3.6. Sample 14LN16-1

This medium-grained garnet-biotite-plagioclase gneiss sample was collected from the Xiaolaihe iron mining area to the southwest of the Qingyuan County (Fig. 2). The biotite-plagioclase gneiss is interlayered with iron-hosting amphibolite (Fig. 3f). The gneiss has a mineral assemblage of garnet (10%) + biotite (5%) + plagioclase (50%) + quartz (30%) + magnetite (5%) (Fig. 4f).

4. Analytical methods

Zircons were extracted from samples by standard mineral separation techniques, and then mounted into epoxy resin and polished to half of their thickness. Prior to zircon U–Pb–Hf analysis, cathodoluminescence (CL) imaging was applied to reveal the internal structures and to identify the potential analytical sites. CL imaging was conducted using a Hitachi S3000N scanning electron microscope equipped with ChromaCL detector at the Beijing SHRIMP Center, Institute of Geology, Chinese Academy of Geological Sciences (IGCAGS).

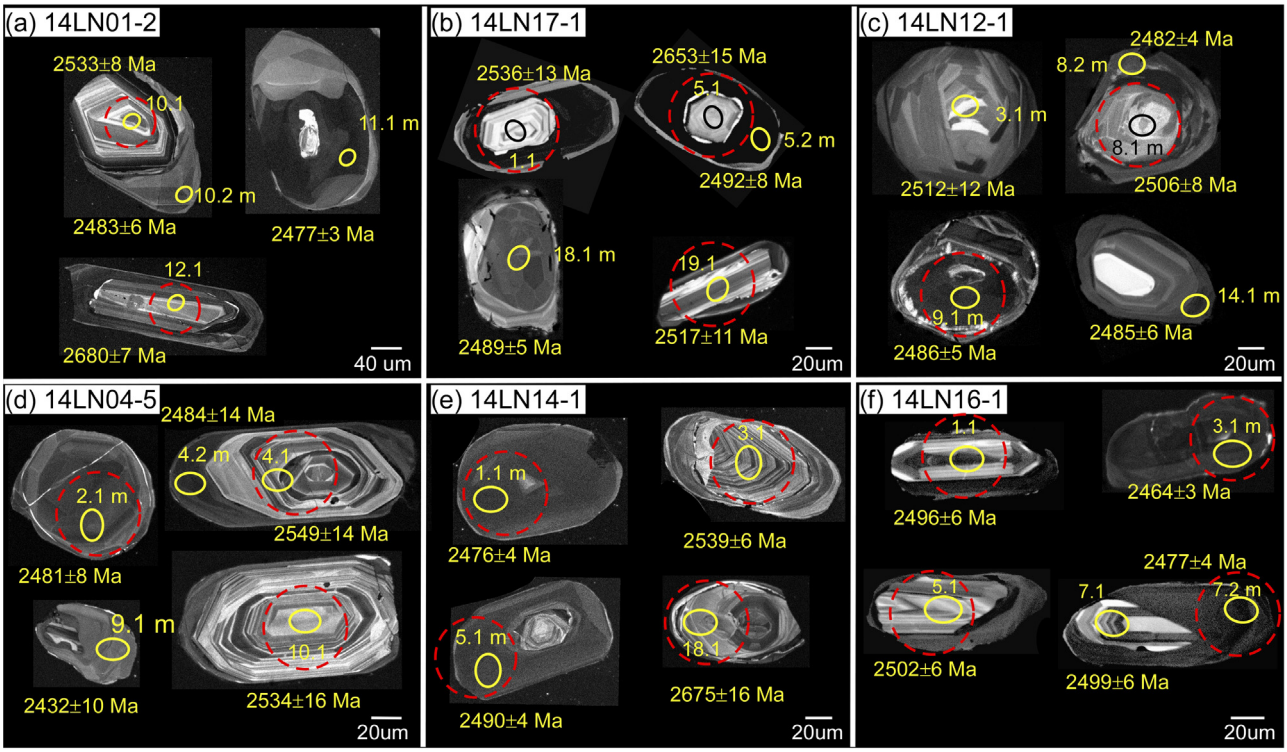

Fig. 5. Cathodoluminescence images (CL) of representative zircons from the Northern Liaoning Complex. The solid circles and dashed circles represent U–Pb and Lu–Hf analytical positions, respectively. U–Pb spot number and apparent $^{207}Pb/^{206}Pb$ ages are indicated.

Zircon U–Pb dating was conducted using the SHRIMP II ion microprobe at the Beijing SHRIMP Center, IGCAGS. The analytical procedures were similar to those described by Williams (1998). The intensity of the primary ^{2-}O ion beam was ~5 nA, and the spot size was around 23 μm. Each analytical site was rastered for 3 min prior to analysis to remove the carbon coating and alteration. Five scans through the nine mass stations were made for each analysis. Reference standard zircons M257 (U = 840 ppm; $^{206}Pb/^{238}U$ age = 562 Ma) (Nasdala et al., 2008) and TEMORA 1 ($^{206}Pb/^{238}U$ age = 417 Ma) (Black et al., 2003) were used for calibration of elemental abundance and $^{206}Pb/^{238}U$, respectively. Every three analyses of unknown were followed by one analysis of TEMORA 1. The measured ^{204}Pb abundances were applied for the common lead correction. Data processing was carried out using the SQUID and ISOPLOT programs (Ludwig, 2003). The zircon U–Th–Pb isotopic data are given in Supplementary Table 1. The uncertainties for the isotopic ratios of individual analyses are quoted at 1σ, whereas uncertainties for weighted mean ages are given at 2σ (95% confidence level).

Supplementary Table 1 related to this article can be found, in the online version, at http://dx.doi.org/10.1016/j.precamres.2015.12.013.

In situ zircon Lu–Hf analyses were performed using a Neptune MC-ICP-MS equipped with a 193-nmArF-excimer laser at the Institute of Geology and Geophysics, Chinese Academy of Sciences (IGGCAS) in Beijing, China. Analytical procedures were described in more detail by Wu et al. (2006). During the whole analyses, a laser beam of 44 μm in diameter with a repetition rate of 8 Hz was adopted. Standard Zircons GJ-1 and Mud Tank were used as reference standards. Repeated measurements on GJ-1 and Mud Tank yielded weighted mean $^{176}Hf/^{177}Hf$ ratios of 0.282013 ± 8 (2σ, n = 30, MSWD = 1.4) and 0.282509 ± 4 (2σ, n = 57, MSWD = 1.9), respectively, which are in good agreement with the recommended values within 2σ error (Morel et al., 2008; Sláma et al., 2008; Xie et al., 2008). Calculation of $\varepsilon_{Hf}(t)$ values was based on the present chondritic uniform reservoir (CHUR) values with $^{176}Hf/^{177}Hf = 0.282785$ and $^{176}Lu/^{177}Hf = 0.0336$ (Bouvier et al., 2008), using the decay constant of ^{176}Lu of 1.867×10^{-11} yr^{-1} (Söderlund et al., 2004). As all the samples were intermediate to acid rocks based on the mineral assemblages, two-stage depleted mantle model (T_{DM2}) ages were adopted throughout this study and calculated with a mean $^{176}Lu/^{177}Hf$ ratio of 0.022 for the lower continental crust (Amelin et al., 1999). All the zircon Lu–Hf isotopic data and calculation details are presented in Supplementary Table 2 with an error of 2σ.

Supplementary Table 2 related to this article can be found, in the online version, at http://dx.doi.org/10.1016/j.precamres.2015.12.013.

5. Results

5.1. Sample 14LN01-2

The zircon morphology and internal structures revealed by CL imaging show that most zircons are subhedral prismatic with rounded terminations, sizing from 150 to 300 μm in length, and have clear core-rim structures (Fig. 5a). The cores are commonly featured by intense oscillatory zoning, indicative of igneous origin. These igneous cores are surrounded or truncated by rims with/without blurred oscillatory zoning. The rims are mainly 20–80 μm in width and were considered to have formed by recrystallization or overgrowth during later metamorphism. Some zircon grains have structureless or complicated dark zone between the core and rim, likely representing the domain where metamorphic recrystallization occurred. A total of twenty-one analyses were performed on seventeen zircon grains, of which twelve were on magmatic domains and nine on metamorphic domains. Ten of the twelve analyses on magmatic zircon domains give younger apparent $^{207}Pb/^{206}Pb$ ages ranging from 2556 Ma to 2495 Ma (Supplementary Table 1), of which six yielded a weighted mean age of

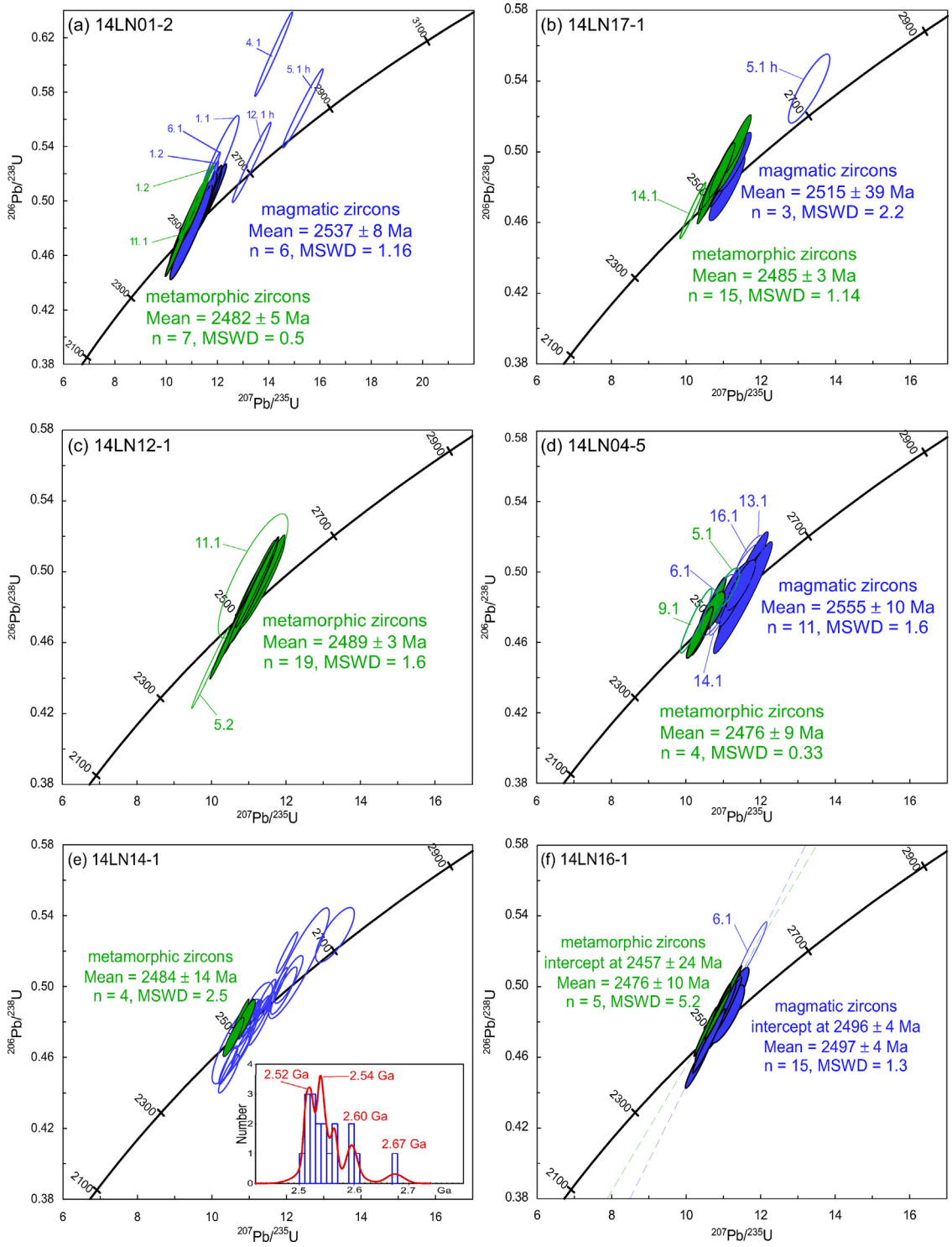

Fig. 6. Concordia diagrams of zircon U–Pb data for the Northern Liaoning Complex. The blue and green circles represent magmatic and metamorphic zircon domains, respectively. Analytical errors are depicted at the 1 sigma level. (For interpretation of the references to color in this figure legend, the reader is referred to the web version of the article.)

2537 ± 8 Ma (MSWD = 1.16; Fig. 6a), representing the crystallization age of the protolith for the granulite. The other two analyses gave older concordant apparent $^{207}Pb/^{206}Pb$ ages of 2791 ± 6 and 2679 ± 7 Ma (Supplementary Table 1), interpreted to be inherited zircons. Seven concordant analyses of the nine analyses on metamorphic domains gave consistent apparent $^{207}Pb/^{206}Pb$ ages of 2490–2476 Ma (Supplementary Table 1), yielding a weighted mean age of 2482 ± 5 Ma (MSWD = 0.5; Fig. 6a). This age is interpreted to be the timing of a metamorphic event in the Northern Liaoning Complex.

The results of Lu–Hf analyses on magmatic zircons show variable $^{176}Lu/^{177}Hf$ ratios of 0.000247–0.001641 and $^{176}Hf/^{177}Hf$ ratios of 0.281144–0.281448 (Supplementary Table 2). The $\varepsilon_{Hf}(t)$ (t = 2537 Ma, weighted mean $^{207}Pb/^{206}Pb$ age of the sample) values range from −3.2 to +8.5 with two-stage depleted mantle Hf model (T_{DM2}) ages ranging from 3.53 to 2.51 Ga (Supplementary Table 2).

Comparatively, the metamorphic zircons have less variable $^{176}Lu/^{177}Hf$ ratios of 0.000381–0.000483 and $^{176}Hf/^{177}Hf$ ratios of 0.281275–0.281437, with $\varepsilon_{Hf}(t)$ (t = 2484 Ma) values from +2.2 to +8.1 and T_{DM2} ages of 3.02–2.72 Ga (Supplementary Table 2).

5.2. Sample 14LN17-1

Zircons from this sample are mainly subhedral prismatic with rounded termination, and the grain size varies from 100 to 150 μm in length. As revealed by CL images, most zircons have thin high-luminescent rims (<30 μm) surrounding cores that can be oscillatory-zoned, patchy-zoned or structureless (Fig. 5b). Many zircons develop low-luminescent zones between the cores and rims, representing recrystallization domains. The oscillatory zoning suggests a magmatic origin, whereas the patchy-zoning and structureless cores as well as the thin recrystallization rims were considered to be of metamorphic origin. Twenty analyses were made on nineteen zircon grains in total, with four on magmatic domains and the remaining on metamorphic domains. Three of the four analyses on the magmatic zircons yielded weighted mean $^{207}Pb/^{206}Pb$ age of 2515 ± 39 Ma (MSWD = 2.2; Fig. 6b). This age is interpreted to represent the protolith age of the granulite, and is identical within error to the crystallization age of sample 14LN01-2 described above. The fourth analysis yielded an older disconcordant apparent $^{207}Pb/^{206}Pb$ age of 2653 ± 15 Ma (spot 5.1 on Fig. 6b), interpreted to be an inherited zircon. Fifteen of the sixteen analyses on metamorphic zircons show apparent $^{207}Pb/^{206}Pb$ ages ranging from 2494 to 2468 Ma with a weighted mean $^{207}Pb/^{206}Pb$ age of 2485 ± 3 Ma (MSWD = 1.14; Fig. 6b). This age is explained as the age of the regional metamorphism.

Magmatic zircons from this sample have variable $^{176}Lu/^{177}Hf$ ratios of 0.000050–0.001196 but relatively homogeneous $^{176}Hf/^{177}Hf$ ratios of 0.281163–0.281412 (Supplementary Table 2). The $\varepsilon_{Hf}(t)$ (t = 2515 Ma) values vary largely from −1.2 to +7.9 with T_{DM2} ages from 3.34 Ga to 2.55 Ga (Supplementary Table 2). Metamorphic zircons show less variable $^{176}Lu/^{177}Hf$ ratios of 0.000381–0.000483 and $^{176}Hf/^{177}Hf$ ratios of 0.281319–0.281470, with $\varepsilon_{Hf}(t)$ (t = 2485 Ma) values from +4.3 to +9.0 and T_{DM2} ages of 2.84–2.43 Ga (Supplementary Table 2).

5.3. Sample 14LN12-1

Zircons extracted from this amphibolite sample are mainly subhedral rounded grains with sizes around 100–120 μm in diameter. Although many zircons have core-rim structure, the cores are generally structureless or sector-zoned, indicative of metamorphic origin. The rims are typical metamorphic recrystallized rims and some grains show structureless recrystallization with low-luminescence (Fig. 5c). Twenty-one analyses on eighteen zircon grains were made with apparent $^{207}Pb/^{206}Pb$ ages of 2512–2459 Ma (Supplementary Table 1), of which nineteen yielded a weighted mean $^{207}Pb/^{206}Pb$ age of 2489 ± 3 Ma (MSWD = 1.6; Fig. 6c). This age is interpreted to be the age of metamorphism and is consistent with the metamorphic ages documented by the granulites.

Metamorphic zircons from this sample have variable $^{176}Lu/^{177}Hf$ ratios of 0.000011–0.000690 but relatively homogeneous $^{176}Hf/^{177}Hf$ ratios of 0.281286–0.281430 (Supplementary Table 2). The $\varepsilon_{Hf}(t)$ (t = 2488 Ma) values vary largely from +3.4 to +9.6 with T_{DM2} ages from 2.92 Ga to 2.39 Ga (Supplementary Table 2).

5.4. Sample 14LN04-5

Zircon grains from this sample show two distinct types based on their morphology and internal structures as revealed by CL imaging. Type A zircons are subhedral prismatic grains with rounded terminations sizing from 120 to 160 μm. These grains commonly have magmatic cores characterized by intensive oscillatory zoning surrounded by metamorphic recrystallized rims (grains in the right of Fig. 5d). Type B zircons are mainly subhedral to anhedral rounded grains sizing from 60 to 80 μm, of which most are structureless whereas some have wide rims truncating relict magmatic cores (grains in the left of Fig. 5d). These structureless domains and rims are indicative of metamorphic origin. Twenty-two analyses in total were made on nineteen grains. One spot hit on the boundary between magmatic and metamorphic domains is excluded from discussion. Fifteen analyses on magmatic domains show apparent $^{207}Pb/^{206}Pb$ ages between 2494 Ma and 2578 Ma, of which eleven yielded a weighted mean $^{207}Pb/^{206}Pb$ age of 2555 ± 10 Ma (MSWD = 1.6; Fig. 6d). This age is considered to be the protolith age of the garnet-biotite-plagioclase gneiss. Six analyses on metamorphic domains gave apparent $^{207}Pb/^{206}Pb$ ages of 2432–2501 Ma, and four of them yielded a weighted mean $^{207}Pb/^{206}Pb$ age of 2476 ± 9 Ma (MSWD = 0.33; Fig. 6d), representing the timing of metamorphism.

The magmatic zircon $^{176}Lu/^{177}Hf$ ratios vary largely from 0.000501 to 0.001408 whereas their $^{176}Hf/^{177}Hf$ ratios vary less significantly from 0.281237 to 0.281427 (Supplementary Table 2). Their $\varepsilon_{Hf}(t)$ (t = 2555 Ma) values and T_{DM2} ages range from +2.3 to +8.6 and 3.07 Ga to 2.52 Ga, respectively (Supplementary Table 2). Metamorphic zircons show variable $^{176}Lu/^{177}Hf$ ratios of 0.000026–0.001280 and $^{176}Hf/^{177}Hf$ ratios of 0.281364–0.281507, with $\varepsilon_{Hf}(t)$ (t = 2476 Ma) values from +5.9 to +9.3 and T_{DM2} ages of 2.69–2.40 Ga (Supplementary Table 2).

5.5. Sample 14LN14-1

Zircons in this garnet-biotite-plagioclase gneiss are generally subhedral to euhedral prismatic with rounded terminations or stubby grains. Most zircon grains are around 100 μm in diameter. Their rounded crystal shape as well as the abundant garnet and biotite contents indicate that this rock is possibly a paragneiss. CL images show that most zircons have magmatic cores with oscillatory zoning surrounded by either magmatic zonation or structureless low-luminescent rims formed during metamorphism (Fig. 5e). A total of twenty-two analyses were performed on twenty-one grains. Eighteen analyses on magmatic domains show apparent $^{207}Pb/^{206}Pb$ ages varying from 2675 Ma to 2505 Ma, most of which fall on or near the concordia (Fig. 6e). This age distribution pattern with several peaks are more likely found in metasedimentary rocks rather than in igneous rocks. Therefore, we interpreted these zircons as detrital zircons. The youngest age of 2505 Ma predates the deposition of the sediments. The magmatic age peaks at ~2.52 Ga, ~2.54 Ga and 2.56–2.60 Ga are consistent with the local magmatic events. These suggest that the protolith of this paragneiss may have been sourced from the local rocks in the studied region. Four analyses on metamorphic domains gave a weighted mean $^{207}Pb/^{206}Pb$ age of 2484 ± 14 Ma (MSWD = 2.5; Fig. 6e), approximating the timing of regional metamorphism. These data constrain the timing of deposition between 2505 Ma and 2484 Ma.

Lu–Hf isotopic analyses of magmatic zircons show a wide range of $^{176}Lu/^{177}Hf$ ratios of 0.000137–0.001609 and $^{176}Hf/^{177}Hf$ ratios of 0.281081–0.281402, with $\varepsilon_{Hf}(t)$ (t = 2527 Ma) values ranging from −4.0 to +7.2 and T_{DM2} ages from 3.59 Ga to 2.62 Ga (Supplementary Table 2). Metamorphic zircons show similar $^{176}Lu/^{177}Hf$ ratios (0.000090–0.001580) and $^{176}Hf/^{177}Hf$ ratios (0.281113–0.281463), with $\varepsilon_{Hf}(t)$ (t = 2484 Ma) values of −5.4 to +6.4 and T_{DM2} ages of 3.68–2.66 Ga (Supplementary Table 2).

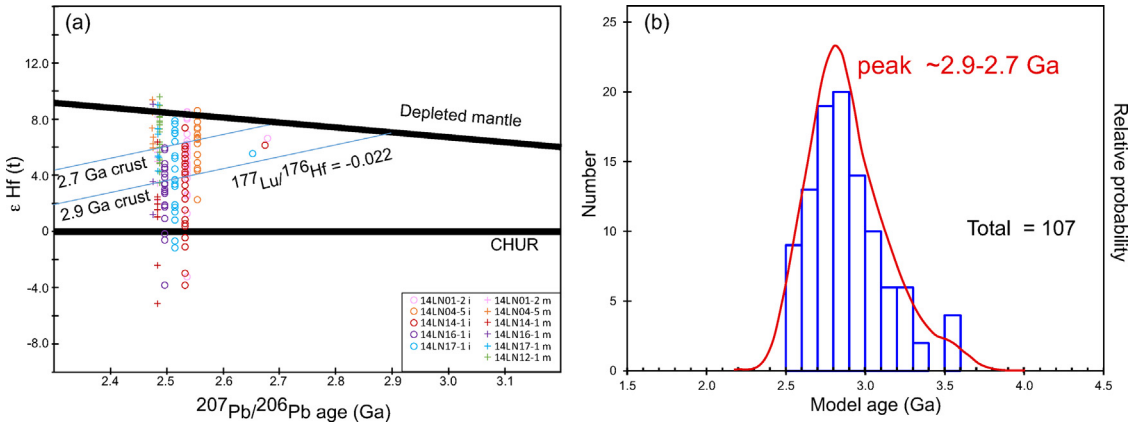

Fig. 7. Results of Lu–Hf analyses for zircons from the Northern Liaoning Complex. (a) $^{207}Pb/^{206}Pb$ ages versus $\varepsilon_{Hf}(t)$ values diagram; (b) histogram of two-stage Hf model ages of magmatic zircons. The suffixes "i" and "m" after the sample numbers in (a) represent magmatic zircons and metamorphic zircons, respectively.

5.6. Sample 14LN16-1

Zircons from this garnet-biotite-plagioclase gneiss are mostly subhedral to euhedral prismatic grains with rounded terminations. Their internal morphology revealed by CL is mainly characterized by magmatic oscillatory zoned cores surrounded by low luminescent metamorphic rims, with some grains showing complete metamorphic recrystallization (Fig. 5f). Twenty-one analyses were made on twenty grains. Sixteen analyses on magmatic zircons cluster tightly and give a weighted mean $^{207}Pb/^{206}Pb$ age of 2497 ± 4 Ma (MSWD = 1.3, Fig. 6f), which is interpreted to be the crystallization age of the protolith magma. Five analyses on metamorphic zircons yielded a weighted mean $^{207}Pb/^{206}Pb$ age of 2476 ± 10 Ma (MSWD = 5.2; Fig. 6f), interpreted to be the age of metamorphism.

Magmatic zircons have $^{176}Lu/^{177}Hf$ ratios from 0.000148 to 0.000758 and $^{176}Hf/^{177}Hf$ ratios from 0.281083 to 0.281561 (Supplementary Table 2). Their $\varepsilon_{Hf}(t)$ (t = 2497 Ma) values vary from −3.8 to +5.9 with T_{DM2} ages of 3.55–2.71 Ga (Fig. 7a, Supplementary Table 2). Metamorphic zircons have $^{176}Lu/^{177}Hf$ ratios of 0.000292–0.000635 and $^{176}Hf/^{177}Hf$ ratios of 0.281242–0.281464, and their $\varepsilon_{Hf}(t)$ (t = 2476 Ma) values vary from +1.2 to +9.0 with T_{DM2} ages from 3.11 Ga to 2.42 Ga (Supplementary Table 2).

6. Discussions

6.1. Tectonothermal framework of the Northern Liaoning Complex

Available zircon U–Pb data for the major lithologies in the Northern Liaoning Complex is summarized in Table 2. In this study, magmatic zircon U–Pb data gave consistent crystallization ages of 2.55–2.50 Ga for the protolith magmas of the granulites and biotite-plagioclase gneisses, in good accordance with previous zircon U–Pb ages of 2.57–2.50 Ga obtained for different lithologies in

Table 2
Summary of zircon U–Pb ages for the Northern Liaoning Complex.

Sample	Rock type	Inherited/detrital zircon age (Ma)	Crystallization age (Ma)	Metamorphic age (Ma)	Source
LQ0107	Amphibole leptynite		2515 ± 6	~2.52 Ga	Wan et al. (2005a)
LF0107	Amphibole leptynite		2510 ± 7		Wan et al. (2005a)
LQ0104	Amphibole leptynite			2479 ± 5	Wan et al. (2005a)
12LN25-2	Amphibolite		2530 ± 5	2507 ± 11	Bai et al. (2014)
P10NC5	Amphibolite			2480 ± 9	Peng et al. (2015)
14NL01-2	Granulite	2791 ± 6 2679 ± 7	2537 ± 8	2482 ± 5	This study
14NL17-1	Granulite	2653 ± 15	2515 ± 39	2485 ± 3	This study
14NL12-1	Amphibolite			2489 ± 3	This study
LQ0110	TTG gneiss		2556 ± 18	2519 ± 48 ~2.47 Ga	Wan et al. (2005a)
LF0106	TTG gneiss		2528 ± 27 2530 ± 22	2477 ± 13	Wan et al. (2005a)
MG-48	Trondhjemite		2553 ± 7	2500 ± 10	Grant et al. (2009)
MG-141	Tonalite		2534 ± 4	2510 ± 7	Grant et al. (2009)
MG-146	Trondhjemite			2497 ± 7	Grant et al. (2009)
13LB49-3	Trondhjemitic gneiss	2674 ± 48	2550 ± 10	2508 ± 49	Bai et al. (2014)
12LN04-1	Tonalitic gneiss		2544 ± 4		Bai et al. (2014)
12LN27-1	Trondhjemitic gneiss		2518 ± 23	2473 ± 30	Bai et al. (2014)
P10PJW1	Tonalite		2526 ± 11		Peng et al. (2015)
P10BHG5	Tonalite		2520 ± 12		Peng et al. (2015)
14NL04-5	Grt-Hb-Bt-Pl gneiss		2555 ± 10	2476 ± 9	This study
14NL14-1	Grt-Bt-Pl gneiss	2675–2505		2484 ± 14	This study
14NL16-1	Grt-Bt-Pl gneiss		2497 ± 4	2476 ± 10	This study
12LN39-3	Quartz dioritic gneiss		2571 ± 7		Bai et al. (2014)
12LN30-2	Quartz diorite		2496 ± 18		Bai et al. (2014)
P10PLH3	Quartz diorite	2661 ± 12	2523 ± 6	2478 ± 18	Peng et al. (2015)
P10YJD3	Quartz monzodiorite		2512 ± 10		Peng et al. (2015)
MG-47	Syenogranite		2502 ± 11	2516 ± 32	Grant et al. (2009)
12LN01-1	Granite		2522 ± 4		Bai et al. (2014)

Mineral abbreviations: Bt – biotite; Grt – garnet; Hb – hornblende; Pl – plagioclase; Qtz – quartz.

the Northern Liaoning Complex (Table 2; Bai et al., 2014; Grant et al., 2009; Peng et al., 2015; Wan et al., 2005a). As shown in Table 2, in general, TTG magmatism and mafic magmatism occurred almost simultaneously during 2.56–2.52 Ga and 2.54–2.51 Ga, respectively. The emplacement of quartz-diorite/monzodiorite extended from 2.57 to 2.50 Ga. Minor post-tectonic potassic magmatism at 2.52–2.50 Ga marks the cession of this magmatic event. In addition, several inherited magmatic cores and detrital zircons from this complex have ages varying from 2.79 Ga to 2.60 Ga (Table 2; Bai et al., 2014; Grant et al., 2009; Peng et al., 2015; Wan et al., 2005a), indicating the existence of older crust in this region. All these zircon U–Pb ages suggest a major magmatic activity in the Northern Liaoning domain during 2.57–2.50 Ga, which is consistent with other complexes in the Eastern Block (e.g. Geng et al., 2006; Nutman et al., 2011; Tang et al., 2007; Wang et al., 2012, 2013a,b; Wu et al., 2013a; Yang et al., 2008).

Metamorphic overgrowth/recrystallization domains of zircons are present in all samples (Fig. 5), indicating that the Northern Liaoning Complex experienced medium- to high-grade regional metamorphism. In this study, we obtained metamorphic zircon ages of 2.49–2.48 Ga, in agreement with previous metamorphic zircon ages of 2.52–2.47 Ga from the Northern Liaoning Complex (Table 2). These indicate that a regional metamorphic event happened immediately after the extensive magmatism (2.57–2.50 Ga) in this region. This ~2.5 Ga metamorphism has also been documented in other Archean complexes in the Eastern Block (e.g. Ge et al., 2003; Geng et al., 2006; Liu et al., 2011; Wan et al., 2012; Wang et al., 2012, 2013a,b; Wu et al., 2013a; Yang et al., 2008; Zhao et al., 1998), suggesting a widespread tectonothermal event over the entire Eastern Block at the end of the Neoarchean.

In summary, available zircon geochronological data indicate that the Northern Liaoning Complex experienced extensive magmatism between 2.57 and 2.50 Ga and immediately encountered strong regional tectonothermal overprinting during 2.52–2.47 Ga. Earlier magmatism may also exist in this region as revealed by inherited zircons of 2.79–2.59 Ga.

6.2. Crustal evolution of the Northern Liaoning Complex

Zircon Lu–Hf system is commonly used to trace the magma origin and constrain the timing of crust–mantle differentiation (Kinny and Maas, 2003; Wu et al., 2007; Zeh et al., 2010). Basic rocks were derived from the depleted mantle through partial melting, whereas the intermediate-acidic rocks were formed by partial melting of the middle-lower crust that originated from the depleted mantle. Basically, the Hf model age that greatly exceeds the magma crystallization age suggests a long crustal residence period after the magma was separated from the depleted mantle. On the other hand, if the Hf model age is close to the crystallization age, the parent rocks are considered to be juvenile with short crustal residence time or mantle-derived rocks. In this study, as most of the samples were intermediate-acidic, two-stage Hf model ages were adopted for discussion by calibration using the Lu/Hf differentiation index ($f_{Lu/Hf}$) of the lower crust to represent the timing when the magma was extracted from the depleted mantle (e.g. Wu et al., 2007).

Zircon Lu–Hf data from the Northern Liaoning Complex is reported and discussed for the first time in this study to decipher the crustal evolution of this complex. As shown on the $\varepsilon_{Hf}(t)$ values versus zircon formation age diagram (Fig. 7a), zircons from all samples preserved variable Hf isotopic compositions against relatively consistent formation ages. For the metamorphic zircons, most $\varepsilon_{Hf}(t)$ values are positive and situated between that of the contemporary depleted mantle and the chondrite, with only two grains showing negative $\varepsilon_{Hf}(t)$ values. As Lu–Hf isotopic system is generally considered to be resistant to the modification of metamorphism and metamorphic zircons from the Northern Liaoning Complex show similar $^{176}Hf/^{177}Hf$ ratios to that of the magmatic zircons (Fig. 7a), it is believed that the Lu–Hf isotopic system was essentially not disturbed during the later metamorphism (Kinny and Maas, 2003; Wu et al., 2007; Zeh et al., 2010). Therefore, these metamorphic zircons inherited the primary Hf signatures from the magmatic zircons.

Magmatic zircons have $\varepsilon_{Hf}(t)$ values varying from −4.0 to +9.0 with T_{DM2} ages of 3.59–2.44 Ga. The majority of the $\varepsilon_{Hf}(t)$ values are positive and situated between the evolutionary trends of the depleted mantle and chondrite (Fig. 7a) with the two-stage model ages peak at 2.9–2.7 Ga (Fig. 7b), suggesting the crust was mainly originated from recycling of the pre-existed 2.9–2.7 Ga juvenile crust at the end of the Neoarchean. A few magmatic zircons with high positive $\varepsilon_{Hf}(t)$ values close to that of the contemporary depleted mantle and model ages close to their formation ages (~2.6–2.5 Ga) indicate that minor juvenile additions also contribute to the crust evolution. In addition, some magmatic zircons with negative $\varepsilon_{Hf}(t)$ values (−4.0 to −0.2) and much older model ages (3.6–3.2 Ga) suggest the involvement of ancient crustal materials, implying the possible existence of Paleoarchean crust in the Northern Liaoning Complex. Collectively, the zircon Lu–Hf isotopic data presented in this study reveal that the Northern Liaoning Complex experienced major juvenile crustal growth with minor additions of older crustal materials at 2.9–2.7 Ga (Fig. 7b), followed by an intensive crustal reworking event with minor juvenile additions at ~2.6–2.5 Ga.

6.3. Implications for the continental crustal evolution of the Eastern Block

Controversy has long surrounded the early crustal evolution of the Eastern Block in the NCC. Based on the large volume of ~2.6–2.5 Ga rocks over the whole Eastern Block and their arc-like geochemical signatures (e.g. Geng et al., 2006; Nutman et al., 2011; Wan et al., 2005a,b; Wang et al., 2012, 2013a,b; Yang et al., 2008), some scholars suggest the major crustal growth occurred at ~2.5 Ga (Diwu et al., 2011; Liu et al., 2009). Conversely, other researchers propose that the major juvenile crustal growth in the Eastern Block occurred during early Neoarchean between 2.9 and 2.7 Ga (Geng et al., 2012; Jiang et al., 2010; Wan et al., 2010; Wang and Liu, 2012). The latter is supported by that the Nd and Hf depleted mantle model ages of the voluminous ~2.5 Ga basement rocks are concentrated at 2.9–2.7 Ga, suggesting the end-Neoarchean crust of the Eastern Block was mostly originated from the reworking of the 2.9–2.7 Ga crust (Geng et al., 2012; Jahn et al., 2008; Jiang et al., 2010; Wan et al., 2010, 2011, 2012; Wang and Liu, 2012; Wu et al., 2005, 2013a, 2014a,c). Such a conclusion is also manifested by the inherited zircons of 2.79–2.60 Ga and the model ages (concentrated between 2.9 Ga and 2.7 Ga) of the late Neoarchean magmatic zircons (2.6–2.5 Ga) from the Northern Liaoning Complex. The Northern Liaoning Complex share similar crustal evolutionary history to other Archean complexes in the Eastern Block, such as the Eastern Hebei Complex (Geng et al., 2006; Yang et al., 2008), the Western Shandong Complex (Wan et al., 2010, 2012; Wang et al., 2013b, 2014; Wu et al., 2012), the Eastern Shandong Complex (Tang et al., 2007; Wu et al., 2014a) and the Western Liaoning Complex (Wang et al., 2012, 2013a). Most recently, the increasing recognitions of ~2.9–2.7 Ga rocks over the Eastern Block, and even over the entire NCC, have further confirmed the existence of the 2.9–2.7 Ga crust (Guan et al., 2002; Jahn et al., 2008; Liu et al., 2009, 2015; Tang et al., 2007; Wan et al., 2011; Wu et al., 2014a,b). Therefore, many researchers have proposed that the early Neoarchean basement (~2.9–2.7 Ga) may be more extensive than now recognized in the Eastern Block and the NCC, whereas the limited exposures may have resulted from the intra-crustal reworking and overprinting by the intensive ~2.5 Ga tectonothermal event at the end of

the Neoarchean (e.g. Jiang et al., 2010; Wan et al., 2011; Wang and Liu, 2012).

The close spatial and temporal relationships between the magmatism and the metamorphism characterize the tectonothermal evolution of the Eastern Block during the Neoarchean. However, neither whole-rock Nd isotopes nor zircon Hf isotopes can be directly correlated to a specific tectonic setting without evidence from petrology, field relationships and geochemistry of the parent rocks. Different models have been proposed to account for the crustal reworking mechanism and geodynamic settings at the end of the Neoarchean over the Eastern Block. Traditionally, some scholars considered the Neoarchean complexes in the Eastern Block as typical Archean granite-greenstone terrains. The high-grade gneiss terrains represent individual micro-continental blocks, and they amalgamated along several greenstone belts to form the Eastern Block, leading to the formation and cratonization of the North China Craton at the end of the Neoarchean (Zhai et al., 1985; Zhai, 2014). On the basis of arc-like geochemical signatures of most Neoarchean complexes in the Eastern Block, Wan et al. (2005a,b) consider that these Archean complexes represent an arc-continent collision at the end of the Neoarchean, and similarly some other scholars propose that these complexes formed in an active continental margin involving subduction and arc magmatism (Liu et al., 2011; Nutman et al., 2011; Wang et al., 2012, 2013a). Most recently, Peng et al. (2015) proposed a mantle wedge-absent flat hot subduction model with synchronous vertical mechanism to explain the origin and tectonic setting of the Northern Liaoning Complex (i.e. the Qingyuan granite-greenstone terrain). All these tectonic models share a common basic assumption that plate tectonics began as early as in the Neoarchean and horizontal mechanism dominated the geodynamic processes during the Neoarchean. Alternatively, vertical mechanism may also play an important role during the Neoarchean. Based on the widespread distribution of the Neoarchean metamorphic complexes in the Eastern Block and the absence of lateral age progression pattern that is typical of an arc system, the Neoarchean crust of Eastern Block may have formed in plume-related settings (Geng et al., 2006; Grant et al., 2009; Wu et al., 2012, 2013a,b, 2014a; Yang et al., 2008; Zhao et al., 2012), either beneath a continent (underplating) to form the lower crust or within an ocean to form an oceanic plateau (e.g. Puchtel et al., 1998). However, further petrological, structural, metamorphic and geochemical studies are required to determine the detailed mechanism of the crustal formation and reworking. Overall, the NCC share similar crustal evolution to many other cratons in the world with significant early Neoarchean (2.9–2.7 Ga) crust–mantle differentiation event (e.g. Condie and Aster, 2010; Condie et al., 2009), although the NCC experienced a distinctive intensive tectonothermal superimposition at ~2.5 Ga.

7. Conclusions

Integration of new zircon U–Pb and Lu–Hf data presented in this study and previous studies for the Northern Liaoning Complex has reached the following main conclusions:

(1) Magmatic zircon U–Pb data suggest that the major lithologies of the Northern Liaoning Complex formed during late Neoarchean between 2.57 Ga and 2.50 Ga.
(2) Metamorphic zircons record a significant regional metamorphic event around 2.52–2.47 Ga, consistent with the widespread tectonothermal events in the Eastern Block.
(3) Zircon Lu–Hf data have revealed a major juvenile crustal growth event during 2.9–2.7 Ga with additions of older crustal materials, whereas crustal recycling was dominant during the 2.6–2.5 Ga tectonothermal event.

Acknowledgements

This research was funded by the National Natural Science Foundation of China (NSFC) Projects (41472166, 41472169), Natural Sciences and Engineering Research Council of Canada (NSERC), and the Key Program of the Ministry of Land and Resources, China (12120114021301). We appreciate the help from Mr. Daheng Ren (Senior Geologist from Liaoning No. 10 Geological Survey Team) during the field work. We thank Drs. Shoujie Liu and Peng Ren from the Beijing SHRIMP Center for their assistance with the zircon U–Pb analysis and Dr. Yueheng Yang from IGGCAS for the help with zircon Lu–Hf analysis.

References

Amelin, Y., Lee, D.C., Halliday, A.N., Pidgeon, R.T., 1999. Nature of the Earth's earliest crust from hafnium isotopes in single detrital zircons. Nature 399, 252–255.
Bai, X., Liu, S., Yan, M., Zhang, L., Wang, W., Guo, R., Guo, B., 2014. Geological event series of Early Precambrian metamorphic complex in South Fushun area, Liaoning Province. Acta Petrol. Sin. 30, 2905–2924.
Bai, X., Liu, S., Guo, R., Wang, W., 2015. Zircon U–Pb–Hf isotopes and geochemistry of two contrasting Neoarchean charnockitic rock series in Eastern Hebei, North China Craton: implications for petrogenesis and tectonic setting. Precambrian Res. 267, 72–93.
Bateman, R., Costa, S., Swe, T., Lambert, D., 2001. Archaean mafic magmatism in the Kalgoorlie area of the Yilgarn Craton, Western Australia: a geochemical and Nd isotopic study of the petrogenetic and tectonic evolution of a greenstone belt. Precambrian Res. 108, 75–112.
Beakhouse, G.P., Lin, S., Kamo, S., 2011. Magmatic and tectonic emplacement of the Pukaskwa batholith, Superior Province, Ontario, Canada. Can. J. Earth Sci. 48, 187–204.
Bibikova, E., Petrova, A., Claesson, S., 2005. The temporal evolution of sanukitoids in the Karelian Craton, Baltic Shield: an ion microprobe U–Th–Pb isotopic study of zircons. Lithos 79, 129–145.
Black, L.P., Kinny, P.D., Sheraton, J.W., Delor, C.P., 1991. Rapid production and evolution of late Archaean felsic crust in the Vestfold Block of East Antarctica. Precambrian Res. 50, 283–310.
Black, L.P., Kamo, S.L., Allen, C.M., et al., 2003. TEMORA 1: a new zircon standard for Phanerozoic U–Pb geochronology. Chem. Geol. 200, 155–170.
Bouvier, A., Vervoort, J.D., Patchett, P.J., 2008. The Lu–Hf and Sm–Nd isotopic composition of CHUR: constraints from unequilibrated chondrites and implications for the bulk composition of terrestrial planets. Earth Planet. Sci. Lett. 273, 48–57.
Condie, K.C., Aster, R.C., 2010. Episodic zircon age spectra of orogenic granitoids: the supercontinent connection and continental growth. Precambrian Res. 180, 227–236.
Condie, K.C., Belousova, E., Griffin, W.L., Sircombe, K.N., 2009. Granitoid events in space and time: constraints from igneous and detrital zircon age spectra. Gondwana Res. 15, 228–242.
Crowley, J.L., 2002. Testing the model of late Archean terrane accretion in southern West Greenland: a comparison of the timing of geological events across the Qarliit nunaat fault, Buksefjorden region. Precambrian Res. 116, 57–79.
Diwu, C., Sun, Y., Guo, A., Wang, H., Liu, X., 2011. Crustal growth in the North China Craton at ~2.5 Ga: evidence from in situ zircon U–Pb ages, Hf isotopes and whole-rock geochemistry of the Dengfeng complex. Gondwana Res. 20, 149–170.
Ge, W.C., Zhao, G.C., Sun, D.Y., Wu, F.Y., Lin, Q., 2003. Metamorphic *P–T* path of the Southern Jilin complex: implications for tectonic evolution of the Eastern Block of the North China Craton. Int. Geol. Rev. 45, 1029–1043.
Geng, Y.S., Liu, F.L., Yang, C.H., 2006. Magmatic event at the end of the Archean in Eastern Hebei Province and its geological implication. Acta Geol. Sin. 80 (6), 819–833.
Geng, Y.S., Du, D.L., Ren, L.D., 2012. Growth and reworking of the early Precambrian continental crust in the North China Craton: constraints from zircon Hf isotopes. Gondwana Res. 21, 517–529.
Grant, M.L., Wilde, S.A., Wu, F., Yang, J., 2009. The application of zircon cathodoluminescence imaging, Th–U–Pb chemistry and U–Pb ages in interpreting discrete magmatic and high-grade metamorphic events in the North China Craton at the Archean/Proterozoic boundary. Chem. Geol. 261, 155–171.
Guan, H., Sun, M., Wilde, S.A., Zhou, X., Zhai, M., 2002. SHRIMP U–Pb zircon geochronology of the Fuping Complex: implications for formation and assembly of the North China Craton. Precambrian Res. 113, 1–18.
Guo, J.H., O'Brien, P.J., Zhai, M.G., 2002. High-pressure granulites in the Sangan area, North China Craton: metamorphic evolution, *P–T* paths and geotectonic significance. J. Metamorph. Geol. 20, 741–756.
Guo, J.H., Sun, M., Zhai, M.G., 2005. Sm–Nd and SHRIMP U–Pb zircon geochronology of high-pressure granulites in the Sanggan area, North China Craton: timing of Paleoproterozoic continental collision. J. Asian Earth Sci. 24, 629–642.
Guo, R., Liu, S., Santosh, M., Li, Q., Bai, X., Wang, W., 2013. Geochemistry, zircon U–Pb geochronology and Lu–Hf isotopes of metavolcanics from eastern Hebei reveal Neoarchean subduction tectonics in the North China Craton. Gondwana Res. 24, 664–686.

Hawkesworth, C., Kemp, A., 2006. Evolution of the continental crust. Nature 443, 811–817.
Jahn, B., Auvray, B., Shen, Q., Liu, D., Zhang, Z., Dong, Y., Ye, X., Zhang, Q., Cornichet, J., Mace, J., 1988. Archean crustal evolution in China: the Taishan complex, and evidence for juvenile crustal addition from long-term depleted mantle. Precambrian Res. 38, 381–403.
Jahn, B.M., Liu, D.Y., Wan, Y.S., Song, B., Wu, J.S., 2008. Archean crustal evolution of the Jiaodong Peninsula, China, as revealed by zircon SHRIMP geochronology, elemental and Nd-isotope geochemistry. Am. J. Sci. 308, 232–269.
Jayananda, M., Moyen, J.F., Martin, H., Peucat, J.J., Auvray, B., Mahabaleswar, B., 2000. Late Archaean (2550–2520 Ma) juvenile magmatism in the Eastern Dharwar craton, southern India: constraints from geochronology, Nd–Sr isotopes and whole rock geochemistry. Precambrian Res. 99, 225–254.
Jiang, N., Guo, J., Zhai, M., Zhang, S., 2010. ~2.7 Ga crust growth in the North China craton. Precambrian Res. 179, 37–49.
Kinny, P.D., Maas, R., 2003. Lu–Hf and Sm–Nd isotope systems in zircon. Rev. Mineral. Geochem. 53, 327–341.
Kröner, A., Cui, W.Y., Wang, S.Q., Wang, C.Q., Nemchin, A.A., 1998. Single zircon ages from high-grade rocks of the Jianping Complex, Liaoning Province, NE China. J. Asian Earth Sci. 16, 519–532.
Kröner, A., Jaeckel, P., Brandl, G., Nemchin, A., Pidgeon, R., 1999. Single zircon ages for granitoid gneisses in the Central Zone of the Limpopo Belt, Southern Africa and geodynamic significance. Precambrian Res. 93, 299–337.
Kusky, T.M., Li, J.H., 2003. Paleoproterozoic tectonic evolution of the North China Craton. J. Asian Earth Sci. 22, 383–397.
Li, J.J., Shen, B.F., Li, S.B., Mao, D.B., 1999. Archaean greenstone belts in northern Liaoning province and southern Jilin province, North China. J. Geol. Miner. Resour. 14, 27–34.
Li, J.J., Shen, B.F., 2000. Geochronology of Precambrian continent crust in Liaoning Province and Jilin Province. Prog. Precambrian Res. 23, 244–249.
Li, S.Z., Zhao, G.C., Sun, M., Wu, F.Y., Hao, D.F., Han, Z.Z., Luo, Y., Xia, X.P., 2005. Deformational history of the Paleoproterozoic Liaohe Group in the Eastern Block of the North China Craton. J. Asian Earth Sci. 24, 654–669.
Li, S.Z., Zhao, G.C., Sun, M., Han, Z.Z., Zhao, G.T., Hao, D.F., 2006. Are the South and North Liaohe Groups of the North China Craton different exotic terranes? Nd isotope constraints. Gondwana Res. 9, 198–208.
Li, S., Zhao, G., Wilde, S.A., Zhang, J., Sun, M., Zhang, G., Dai, L., 2010. Deformation history of the Hengshan–Wutai–Fuping Complexes: implications for the evolution of the Trans-North China Orogen. Gondwana Res. 18, 611–631.
Liu, F., Guo, J., Lu, X., Diwu, C., 2009. Crustal growth at ~2.5 Ga in the North China Craton: evidence from whole-rock Nd and zircon Hf isotopes in the Huai'an gneiss terrane. Chin. Sci. Bull. 54, 4704–4713.
Liu, L., Yang, X., Santosh, M., Aulbach, S., 2015. Neoarchean to Paleoproterozoic continental growth in the southeastern margin of the North China Craton: geochemical, zircon U–Pb and Hf isotope evidence from the Huoqiu complex. Gondwana Res. 28, 1002–1018.
Liu, J., Liu, F., Ding, Z., Liu, C., Yang, H., Liu, P., Wang, F., Meng, E., 2013. The growth, reworking and metamorphism of early Precambrian crust in the Jiaobei terrane, the North China Craton: constraints from U–Th–Pb and Lu–Hf isotopic systematics, and REE concentrations of zircon from Archean granitoid gneisses. Precambrian Res. 224, 287–303.
Liu, S., Santosh, M., Wang, W., Bai, X., Yang, P., 2011. Zircon U–Pb chronology of the Jianping Complex: implications for the Precambrian crustal evolution history of the northern margin of North China Craton. Gondwana Res. 20, 48–63.
Lu, S., Zhao, G., Wang, H., Hao, G., 2008. Precambrian metamorphic basement and sedimentary cover of the North China Craton: a review. Precambrian Res. 160, 77–93.
Ludwig, K.R., 2003. ISOPLOT 3.0: A Geochronological Toolkit for Microsoft Excel, vol. 4. Berkeley Geochronology Center Special Publication.
Morel, M.L.A., Nebel, O., Nebel-Jacobsen, Y.J., Miller, J.S., Vroon, P.Z., 2008. Hafnium isotope characterization of the GJ-1 zircon reference material by solution and laser-ablation MC-ICPMS. Chem. Geol. 255, 231–235.
Nasdala, L., Hofmeister, W., Norberg, N., Mattinson, J.M., et al., 2008. Zircon M257 – a homogeneous natural reference material for the ion microprobe U–Pb analysis of zircon. Geostand. Geoanal. Res. 32, 247–265.
Nutman, A.P., Wan, Y., Du, L., Friend, C.R., Dong, C., Xie, H., Wang, W., Sun, H., Liu, D., 2011. Multistage late Neoarchaean crustal evolution of the North China Craton, eastern Hebei. Precambrian Res. 189, 43–65.
Peng, P., Wang, C., Wang, X., Yang, S., 2015. Qingyuan high-grade granite–greenstone terrain in the Eastern North China Craton: root of a Neoarchaean arc. Tectonophysics 662, 7–21.
Peng, T., Fan, W., Peng, B., 2012. Geochronology and geochemistry of late Archean adakitic plutons from the Taishan granite–greenstone Terrain: implications for tectonic evolution of the eastern North China Craton. Precambrian Res. 208–211, 53–71.
Percival, J., Sanborn-Barrie, M., Skulski, T., Stott, G., Helmstaedt, H., White, D., 2006. Tectonic evolution of the western Superior Province from NATMAP and Lithoprobe studies. Can. J. Earth Sci. 43, 1085–1117.
Peucat, J.J., Jahn, B.M., 1986. A precise zircon U–Pb age of tonalite from the Archaean granite-greenstone belt in Qingyuan area, Northeast China. Paper Collection of International Conference of Precambrian Crustal Evolution, Beijing, pp. 222–229.
Poujol, M., Robb, L., Anhaeusser, C., Gericke, B., 2003. A review of the geochronological constraints on the evolution of the Kaapvaal Craton, South Africa. Precambrian Res. 127, 181–213.
Puchtel, I.S., Hofmann, A.W., Mezger, K., Jochum, K.P., Shchipansky, A.A., Samsonov, A.V., 1998. Oceanic plateau model for continental crustal growth in the Archaean: a case study from the Kostomuksha greenstone belt, NW Baltic Shield. Earth Planet. Sci. Lett. 155, 57–74.
Rino, S., Komiya, T., Windley, B.F., Katayama, I., Motoki, A., Hirata, T., 2004. Major episodic increases of continental crustal growth determined from zircon ages of river sands: implications for mantle overturns in the Early Precambrian. Phys. Earth Planet. Inter. 146, 369–394.
Santosh, M., 2010. Assembling North China Craton within the Columbia supercontinent: the role of double-sided subduction. Precambrian Res. 178, 149–167.
Shen, B., Luo, H., Han, G., Dai, X., Jin, W., Hu, X., Li, S., Bi, S., 1994. Archean Geology and Metallization in North Liaoning Province and South Jilin Province. Geological Publishing House, Beijing, pp. 1–255.
Shen, Q.H., Zhao, Z.R., Song, B., Song, H.X., 2007. Geology, petrology and SHRIMP zircon U–Pb dating of the Mashan and Xueshan granitoids in Yishui county, Shandong Province. Geol. Rev. 53, 180–186.
Sláma, J., Košler, J., Condon, D.J., Crowley, J.L., et al., 2008. Plešovice zircon – a new natural reference material for U–Pb and Hf isotopic microanalysis. Chem. Geol. 249, 1–35.
Söderlund, U., Patchett, P.J., Vervoort, J.D., Isachsen, C.E., 2004. The ^{176}Lu decay constant determined by Lu–Hf and U–Pb isotope systematics of Precambrian mafic intrusions. Earth Planet. Sci. Lett. 219, 311–324.
Tam, P.Y., Zhao, G.C., Liu, F.L., Zhou, X.W., Sun, M., Li, S.Z., 2011. SHRIMP U–Pb zircon ages of high-pressure mafic and pelitic granulites and associated rocks in the Jiaobei massif: constraints on the metamorphic ages of the Paleoproterozoic Jiao-Liao-Ji Belt in the North China Craton. Gondwana Res. 19, 150–162.
Tang, J., Zheng, Y.F., Wu, Y.B., Gong, B., Liu, X.M., 2007. Geochronology and geochemistry of metamorphic rocks in the Jiaobei terrane: constraints on its tectonic affinity in the Sulu orogen. Precambrian Res. 152, 48–82.
Wan, Y.S., Song, B., Yang, C., Liu, D.Y., 2005a. Zircon SHRIMP U–Pb geochronology of Archaean rocks from the Fushun-Qingyuan area, Liaoning Province and its geological significance. Acta Geol. Sin. 79, 78–87.
Wan, Y.S., Song, B., Geng, Y.S., Liu, D.Y., 2005b. Geochemical characteristics of Archaean basement in the Fushun-Qingyuan area, Northern Liaoning Province and its geological significance. Geol. Rev. 51, 128–137.
Wan, Y.S., Liu, D.Y., Wang, S.J., Dong, C.Y., Yang, E.X., Wang, W., Zhou, H.Y., Du, L.L., Yin, X.Y., Xie, H.Q., Ma, M.Z., 2010. Juvenile magmatism and crustal recycling at the end of Neoarchean in western Shandong Province, North China Craton: evidence from SHRIMP zircon dating. Am. J. Sci. 310, 1503–1552.
Wan, Y.S., Liu, D.Y., Wang, S.J., Yang, E.X., Wang, W., Dong, C.Y., Zhou, H.Y., Du, L.L., Yang, Y.H., Diwu, C.R., 2011. ~2.7 Ga juvenile crust formation in the North China Craton (Taishan-Xintai area, western Shandong Province): further evidence of an understated event from zircon U–Pb dating and Hf isotope composition. Precambrian Res. 186, 169–180.
Wan, Y.S., Wang, S.J., Liu, D.Y., Wang, W., Kröner, A., Dong, C.Y., Yang, E.X., Zhou, H.Y., Xie, H.Q., Ma, M.Z., 2012. Redefinition of depositional ages of Neoarchean supracrustal rocks in western Shandong Province, China: SHRIMP U–Pb zircon dating. Gondwana Res. 21, 768–784.
Wang, A.D., Liu, Y.C., 2012. Neoarchean (2.5–2.8 Ga) crustal growth of the North China Craton revealed by zircon Hf isotope: a synthesis. Geosci. Front. 3, 147–173.
Wang, W., Liu, S.W., Wilde, S.A., Li, Q.G., Zhang, J., Xiang, B., Yang, P.T., Guo, R.R., 2012. Petrogenesis and geochronology of Precambrian granitoid gneisses in Western Liaoning Province: constraints on Neoarchean to early Paleoproterozoic crustal evolution of the North China Craton. Precambrian Res. 222–223, 290–311.
Wang, W., Liu, S., Santosh, M., Bai, X., Li, Q., Yang, P., Guo, R., 2013a. Zircon U–Pb–Hf isotopes and whole-rock geochemistry of granitoid gneisses in the Jianping gneissic terrane, Western Liaoning Province: constraints on the Neoarchean crustal evolution of the North China Craton. Precambrian Res. 224, 184–221.
Wang, W., Zhai, M., Wang, S., Santosh, M., Du, L., Xie, H., Lü, B., Wan, Y., 2013b. Crustal reworking in the North China Craton at ~2.5 Ga: evidence from zircon U–Pb age, Hf isotope and whole rock geochemistry of the felsic volcano-sedimentary rocks from the western Shandong Province. Geol. J. 48, 406–428.
Wang, W., Zhai, M.-G., Tao, Y.-B., Santosh, M., Lü, B., Zhao, L., Wang, S.-J., 2014. Late Neoarchean crustal evolution of the eastern North China Craton: a study on the provenance and metamorphism of paragneiss from the Western Shandong Province. Precambrian Res. 255 (Part 2), 583–602.
Wang, Y., Zhang, Y., Zhao, G., Fan, W., Xia, X., Zhang, F., Zhang, A., 2009. Zircon U–Pb geochronological and geochemical constraints on the petrogenesis of the Taishan sanukitoids (Shandong): implications for Neoarchean subduction in the Eastern Block, North China Craton. Precambrian Res. 174, 273–286.
Wilde, S.A., Zhao, G.C., 2005. Archean to Paleoproterozoic evolution of the North China Craton. J. Asian Earth Sci. 24, 519–522.
Williams, I.S., 1998. U–Th–Pb geochronology by ion microprobe. In: McKibben, M.A., Shanks, W.C., Ridley, W.I. (Eds.), Applications of Microanalytical Techniques to Understanding Mineralizing Processes: Review Economic Geology, vol. 7, pp. 1–35.
Wu, F.Y., Zhao, G.C., Wilde, S.A., Sun, D.Y., 2005. Nd isotopic constraints on crustal formation in the North China Craton. J. Asian Earth Sci. 24, 523–545.
Wu, F.Y., Yang, Y.H., Xie, L.W., Yang, J.H., Xu, P., 2006. Hf isotopic compositions of the standard zircons and baddeleyites used in U–Pb geochronology. Chem. Geol. 234, 105–126.
Wu, Y.B., Zheng, Y.F., Zhang, S.B., Zhao, Z.F., Wu, F.Y., Liu, X.M., 2007. Zircon U–Pb ages and Hf isotope compositions of migmatite from the North Dabie terrane in China: constraints on partial melting. J. Metamorph. Geol. 25, 99–1009.
Wu, M., Zhao, G., Sun, M., Yin, C., Li, S., Tam, P., 2012. Petrology and *P–T* path of the Yishui mafic granulites: implications for tectonothermal evolution of the

Western Shandong Complex in the Eastern Block of the North China Craton. Precambrian Res. 222–223, 312–324.
Wu, M., Zhao, G., Sun, M., Li, S., He, Y., Bao, Z., 2013a. Zircon U–Pb geochronology and Hf isotopes of major lithologies from the Yishui Terrane: implications for the crustal evolution of the Eastern Block, North China Craton. Lithos 170–171, 164–178.
Wu, M., Zhao, G., Sun, M., Li, S., Bao, Z., Tam, P.Y., Eizenhöefer, P.R., He, Y., 2014a. Zircon U–Pb geochronology and Hf isotopes of major lithologies from the Jiaodong Terrane: implications for the crustal evolution of the Eastern Block of the North China Craton. Lithos 190–191, 71–84.
Wu, M., Zhao, G., Sun, M., Bao, Z., Tam, P.Y., He, Y., 2014b. Tectonic affinity and reworking of the Archaean Jiaodong Terrane in the Eastern Block of the North China Craton: evidence from LA-ICP-MS U–Pb zircon ages. Geol. Mag. 151, 365–371.
Wu, M., Zhao, G., Sun, M., Li, S., 2014c. A synthesis of geochemistry and Sm–Nd isotopes of Archean granitoid gneisses in the Jiaodong Terrane: constraints on petrogenesis and tectonic evolution of the Eastern Block, North China Craton. Precambrian Res. 255, 885–899.
Wu, K.K., Zhao, G., Sun, M., Yin, C., He, Y., Tam, P.Y., 2013b. Metamorphism of the northern Liaoning Complex: implications for the tectonic evolution of Neoarchean basement of the Eastern Block, North China Craton. Geosci. Front. 4, 305–320.
Xie, L., Zhang, Y., Zhang, H., Sun, J., Wu, F., 2008. In situ simultaneous determination of trace elements, U–Pb and Lu–Hf isotopes in zircon and baddeleyite. Chin. Sci. Bull. 53, 1565–1573.
Yang, J.H., Wu, F.Y., Wilde, S.A., Zhao, G.C., 2008. Petrogenesis and geodynamics of Late Archean magmatism in eastern Hebei, eastern North China Craton: geochronological, geochemical and Nd–Hf isotopic evidence. Precambrian Res. 167, 125–149.
Yin, C., Zhao, G., Sun, M., Xia, X., Wei, C., Leung, W.H., 2009. LA-ICP-MS U–Pb zircon ages of the Qianlishan Complex: constrains on the evolution of the Khondalite Belt in the Western Block of the North China Craton. Precambrian Res. 174, 78–94.
Yin, C., Zhao, G., Guo, J., Sun, M., Xia, X., Zhou, X., Liu, C., 2011. U–Pb and Hf isotopic study of zircons of the Helanshan Complex: constrains on the evolution of the Khondalite Belt in the Western Block of the North China Craton. Lithos 122, 25–38.
Zeh, A., Gerdes, A., Will, T.M., Frimmel, H., 2010. Hafnium isotope homogenization during metamorphic zircon growth in amphibolite-facies rocks, examples from the Shackleton Range (Antarctica). Geochim. Cosmochim. Acta 74, 4740–4758.
Zhai, M., Yang, R., Lu, W., Zhou, J., 1985. Geochemistry and evolution of the Qingyuan Archean granite greenstone terrain, NE China. Precambrian Res. 27, 37–62.
Zhai, M., 2014. Multi-stage crustal growth and cratonization of the North China Craton. Geosci. Front. 5, 457–469.
Zhang, J., Zhao, G., Sun, M., Wilde, S.A., Li, S., Liu, S., 2006. High-pressure mafic granulites in the Trans-North China Orogen: tectonic significance and age. Gondwana Res. 9, 349–362.
Zhang, J., Zhao, G., Li, S., Sun, M., Liu, S., Wilde, S.A., Kroner, A., Yin, C., 2007. Deformation history of the Hengshan Complex: implications for the tectonic evolution of the Trans-North China Orogen. J. Struct. Geol. 29, 933–949.
Zhang, J., Zhao, G., Li, S., Sun, M., Liu, S., Yin, C., 2009. Deformational history of the Fuping Complex and new U–Th–Pb geochronological constraints: implications for the tectonic evolution of the Trans-North China Orogen. J. Struct. Geol. 31, 177–193.
Zhao, G., Cawood, P.A., 2012. Precambrian geology of China. Precambrian Res. 222–223, 13–54.
Zhao, G., Wilde, S., Cawood, P., Lu, L., 1998. Thermal evolution of Archean basement rocks from the Eastern part of the North China Craton and its bearing on tectonic setting. Int. Geol. Rev. 40, 706–721.
Zhao, G., Wilde, S.A., Cawood, P.A., Sun, M., 2001. Archean blocks and their boundaries in the North China Craton: lithological, geochemical, structural and *P–T* path constraints and tectonic evolution. Precambrian Res. 107, 45–73.
Zhao, G., Sun, M., Wilde, S.A., Li, S., 2005. Late Archean to Paleoproterozoic evolution of the North China Craton: key issues revisited. Precambrian Res. 136, 177–202.
Zhao, G., Cawood, P.A., Li, S., Wilde, S.A., Sun, M., Zhang, J., He, Y., Yin, C., 2012. Amalgamation of the North China Craton: key issues and discussion. Precambrian Res. 222–223, 55–76.
Zhou, X.W., Zhao, G.C., Wei, C.J., Geng, Y.S., Sun, M., 2008. EPMA U–Th–Pb monazite and SHRIMP U–Pb zircon geochronology of high-pressure pelitic granulites in the Jiaobei massif of the North China Craton. Am. J. Sci. 308, 328–350.